Integration simulation method concerning speed control of ultrasonic motor

R Miyauchi[1], B Yue[2] , N Matsunaga[1] and S Ishizuka[1]

[1] Cybernet Systems Co., Ltd. 3 Kanda-neribeicho,Chiyoda-ku, Tokyo,101-0022,Japan
[2] Maplesoft 615 Kumpf Drive Waterloo, ON, N2V 1K8,Canada
E-mail: miya-r@cybernet.co.jp

Abstract. In this paper, the configuration of control system of the ultrasonic motor (USM) from finite element method (FEM) model by applying the nonlinear model order reduction (MOR) is proposed. First, the USM and the FEM model is introduced. Second, FEM model order reduction method is described. Third, the result of comparing the computing time and accuracy of the FEM model and reduced order model is shown. Finaly, nominal model for control is derived by system identification from reduced order model. Nonlinear model predictive control (NMPC) is applied to the nominal model, and speed is controlled. the controller effect is comfirmed by applying the proposed reduced order model.

1. Introduction

Ultrasonic motors (USM) are used widely in the field of Mechatronics. For concrete application, it has been applied to the auto-focus mechanism of a camera, XY tables with linear motion and the robotics in the past [1]. USM is an actuator which is powered by ultrasonic vibration and friction. Its history is still recent compared with the electromagnetic motor. In order to use friction to the rotation drive, the prediction of exact performance is difficult. There are research of modelling of the ultrasonic motor using FEM [2] and the mathematical expression [3]. However, in the stator and the rotor of the contact problem, regarding one as a rigid body, the interaction of the contact is not considered correctly. In this study, reduced order model considering the contact interaction has been proposed. USM control is difficult because of the nonlinearity due to friction drive.

In recent years, attention has been paid to nonlinear model predictive control (NMPC) [4]. On the other hand, there is research which is applied sliding mode control and H∞ control the ultrasonic motor [5] [6]. However, the study of applying model predictive control to the ultrasonic motor has not been confirmed. To apply this method, low-order and high accuracy model is needed. Though FEM simulation is good for the precision result, it is high-order as a plant model for NMPC. Therefore it can not be used as it is.

In this paper, the method of deriving the control model from the finite element model systematic and control system is proposed, and the effectiveness is reported based on simulation.

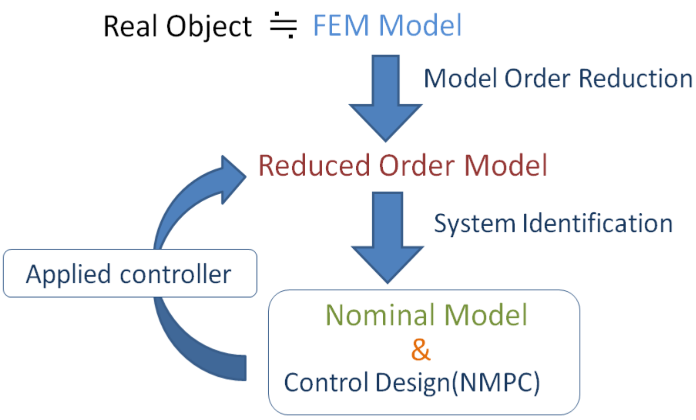

Figure 1. Outline of the paper

Figure 1 shows the outline of the paper. This paper consists of 7 Chapters. Chapter 2 describes the structure of the ultrasonic motor and an overview of FEM model. Chapter 3 describes how to reduced FEM model of the USM. In Chapter 4, the finite element method model and proposed reduced order model are compared about computing time and accuracy. In Chapter 5, it is derived a nominal model of control from the result of proposed reduced order model to build a control system. In order to confirm the effect, the simulation of the control system is performed. Chapter 6 reports conclution. Chapter 7 describes the future work.

Table 1. Comparison by model type

Model Type	Accuracy of model	Computation Time	Control Design
FEM Model	◎	**Very long**	×
Reduced Order Model	○	**Short**	×
Nominal Model	△	**Very short**	◎

Table 1 shows the characteristics of the model appearing in the paper. Double circle FEM model indicates the best performance, single circle intermediate performance, triangle mark lower performance. However, since the computation time is very short, the nominal model is excellent as a plant model for control design while for the other two models cross marks show that they can not be used as a model for constituting a NMPC control system.

2. Ultrasonic motor's FEM model

2.1. The reason for starting from a FEM model

FEM is a strong method to model the real object in detail. In order to predict the performance without using the actual model as much as possible, it is necessary to obtain a model that closely approximates the actual model. If there is a method to obtain a simple model for control system from the model that is thought to approximate the actual model better systematically, it is effective in control design. Therefore, a way to obtain the model of control system by model order reduction (MOR) from FEM model is proposed.

2.2. Drive principle of ultrasonic motor

The structure of USM is explained concisely. When the voltage alternating current is given to a piezoelectric element of ultrasonic motor, travelling wave as in figure 2 (b) is generated. Travelling wave as in figure 2 (a) is also generated in the teeth of USM stator by influence of piezoelectric elements. When the heed is paid to the teeth of the USM stator, its orbit is elliptical. The rotor of USM is rotated by the friction caused by elliptical orbit of the stator.

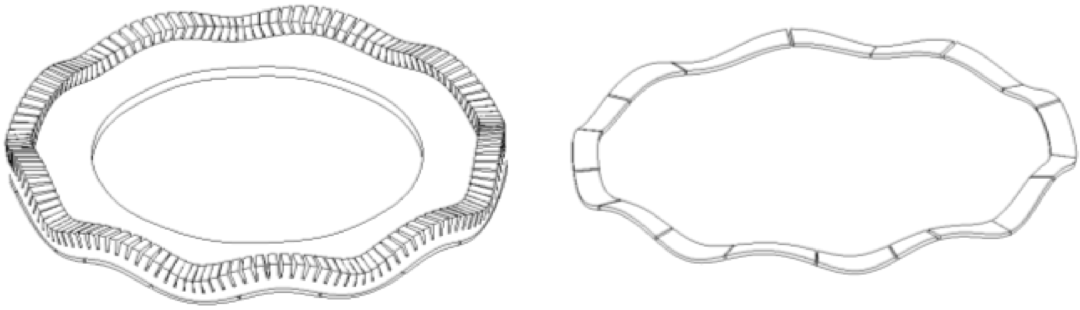

(a) (b)

Figure 2. (a) Travelling wave in the stator and (b) only piezoelectric element

2.3. Finite Element model of ultrasonic motor

Figure 3 (a) shows the finite element model of the USM created by the commercial software ANSYS. It's difficult to simulate drive of ultrasonic motor by FEM. If the contact analysis and the finite deformation have been considered in FEM analysis, it is the nonlinear analysis. Therefore, the calculation time is very long. This section briefly describes how to simulate the travelling-wave-type USM in FEM.

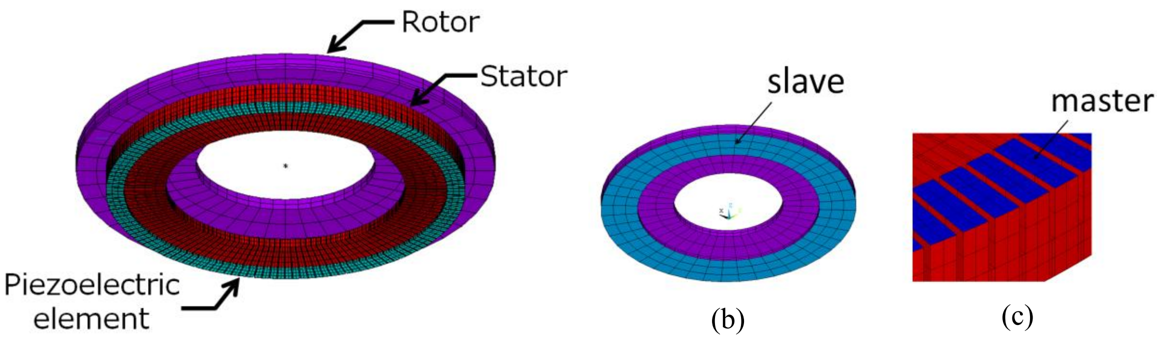

(a) (b) (c)

Figure 3. (a) FEM model (b) FEM contact slave (light blue) and (c) FEM contact master (blue)

Simulation for rotating the USM rotor by ultrasonic vibration requres transient analysis. Configuration of the contacts shown in figure 3 (b) and figure 3 (c) is required between the stator and rotor . Figure 3 (b) shows the slave of the contact, which is set to the rotor. Similarly, figure 3 (c) shows the master of the contact set in the top of the teeth of the stator. Friction coefficient is set to 0.5. To turn the rotor in the friction, The rotor is pressed against the stator with the constant force(10N). From this state, FEM model is generating ultrasonic vibration by applying a voltage to the piezoelectric element of the stator. Therefore, since the friction in this pair of two surfaces occurs, the rotor is rotated. AC voltage of 49 KHz is set to 100V. FEM model have 22,890 nodes and 14,822 elements. This frequency corresponds to the eigen-value of the stator. There are 144 teeth of stator.

Table 2. FEM model geometric properties

Stator(mm)		Stator teeth(mm)		Rotor (mm)		Piezoelectric(mm)
Inner radius	20	**Teeth side**	0.942	**Inner radius**	15	37
Outer radius	30	**Teeth length**	3	**Outer radius**	35	30
Thickness	2	**Height**	2	**Thickness**	3	0.5

Table 3. FEM model Material properties without piezoelectric matrix

	Young Modulus (MPa)	Poisson ratio	Density (Tonne/mm^3)
Stator	170	0.3	2.33E-9
Rotor	7	0.34	2.7E-9

Table 4. Piezoelectric matrix

	Elastic matrix (m^2/N)							**Piezo matrix** (m/V)		
	x	**y**	**z**	**xy**	**yz**	**zx**		**x**	**y**	**z**
x	1.58E-11	-5.7E-12	-7E-12				**x**	0	0	-2.07E-10
y		1.58E-11	-7E-12				**y**	0	0	-2.07E-10
z			1.81E-11				**z**	0	0	4.1E-10
xy				4.3E-11			**xy**	0	0	0
yz					4.06E-11		**yz**	0	5.5E-10	0
zx						4.06E-11	**zx**	5.5E-10	0	0

Table 5. Piezoelectric model Material properties

Density (Tonne/mm^3)
7.7E-9

	Relative Permittivity (-)		
	x	**y**	**z**
x	1087.6		
y		1087.6	
z			1087.6

Table 2 summarizes the dimensions of the stator and the rotor. Table 3 shows the material property values of the stator and the rotor, excluding the piezoelectric element. Table 4 indicates the material properties value of the piezoelectric element of the stator. They are elastic compliance matrix and the piezoelectric matrix. Table5 describes the density and the relative permittivity of piezoelectric element.

3. Model Order Reduction of FEM model

3.1. Purpose of Model Order Reduction

It is possible to create the model for control directly from the result of FEM analysis. However, FEM analysis requires a lot of time, and it is difficult to derive the model for control in a single FEM analysis. Usually it is necessary to obtain data from numerous FEM analyses. It needs a great deal of time. Therefore, to derive the reduced order model and to determine the control model from results of reduced order model are proposed. Methods for obtaining reduced order model of USM is given.

3.2. Piezoelectric equation

The piezoelectric effect is expressed in the following equation. Here, $\boldsymbol{S}$ is strain, $\boldsymbol{T}$ is stress, $\boldsymbol{E}$ is electric field, and $\boldsymbol{D}$ is electric flux density.

$$\begin{cases}\boldsymbol{S} = \boldsymbol{s}^{\boldsymbol{E}}\boldsymbol{T} + \boldsymbol{dE} \\ \boldsymbol{D} = \boldsymbol{d}^{\boldsymbol{T}}\boldsymbol{T} + \boldsymbol{\varepsilon E}\end{cases} \tag{1}$$

Where, $\boldsymbol{s}^{\boldsymbol{E}}$ is the elastic compliance matrix when the electric field strength is fixed. $\boldsymbol{d}$ is the piezoelectric strain matrix. $\boldsymbol{\varepsilon}$ is the permittivity matrix when a stress is fixed. Equation (1) is a piezoelectric equation expressed in the D form.

3.3. Mode reduction to stator model including a piezoelectric effect

Mode reduction is applied to the stator FEM model part of USM [5]. That vibrates small deformation. Therefore, part of this FEM model is linear, and it can be applied mode reduction. If the finite elements of the piezoelectric effect are included in the stator, equation of motion is expressed as follows.

$$\begin{bmatrix} M & 0 \\ 0 & 0 \end{bmatrix}\begin{bmatrix} \ddot{\boldsymbol{u}} \\ \ddot{\boldsymbol{\phi}} \end{bmatrix} + \begin{bmatrix} K_{uu} & K_{u\phi} \\ K_{u\phi}^{T} & K_{\phi\phi} \end{bmatrix}\begin{bmatrix} \boldsymbol{u} \\ \boldsymbol{\phi} \end{bmatrix} = \begin{bmatrix} \boldsymbol{F} \\ \boldsymbol{Q} \end{bmatrix} \tag{2}$$

Where, M is mass matrix, K is stiffness matrix. $\boldsymbol{u}$ and $\boldsymbol{\phi}$ are degrees of freedom. Each $\boldsymbol{u}$ and $\boldsymbol{\phi}$is displacement and electric potential. The voltage is applied as the input condition to the piezoelectric elements. Therefore, equation (2) is transformed as follows. $\overline{\boldsymbol{\phi}}$ is the electric potential degree of freedom.

$$\begin{bmatrix} M & 0 & 0 \\ 0 & 0 & 0 \\ 0 & 0 & 0 \end{bmatrix}\begin{bmatrix} \ddot{\boldsymbol{u}} \\ \ddot{\boldsymbol{\phi}} \\ \ddot{\overline{\boldsymbol{\phi}}} \end{bmatrix} + \begin{bmatrix} K_{uu} & K_{u\phi} & K_{u\overline{\phi}} \\ K_{u\phi}^{T} & K_{\phi\phi} & K_{\phi\overline{\phi}} \\ K_{u\overline{\phi}}^{T} & K_{\phi\overline{\phi}}^{T} & K_{\overline{\phi}\overline{\phi}} \end{bmatrix}\begin{bmatrix} \boldsymbol{u} \\ \boldsymbol{\phi} \\ \overline{\boldsymbol{\phi}} \end{bmatrix} = \begin{bmatrix} \boldsymbol{F} \\ \boldsymbol{0} \\ \boldsymbol{0} \end{bmatrix} \tag{3}$$

Equation (3) is transformed as follows.

$$\begin{bmatrix} M & 0 \\ 0 & 0 \end{bmatrix}\begin{bmatrix} \ddot{\boldsymbol{u}} \\ \ddot{\boldsymbol{\phi}} \end{bmatrix} + \begin{bmatrix} K_{uu} & K_{u\phi} \\ K_{u\phi}^{T} & K_{\phi\phi} \end{bmatrix}\begin{bmatrix} \boldsymbol{u} \\ \boldsymbol{\phi} \end{bmatrix} = \begin{bmatrix} -K_{u\overline{\phi}}\overline{\boldsymbol{\phi}} \\ -K_{\phi\overline{\phi}}\overline{\boldsymbol{\phi}} \end{bmatrix} + \begin{bmatrix} \boldsymbol{F} \\ \boldsymbol{0} \end{bmatrix} \tag{4}$$

A vector of zeros is applied to the right side of equation (4) and eigenvalue analysis is performed.

$$\begin{bmatrix} M & 0 \\ 0 & 0 \end{bmatrix}\begin{bmatrix} \ddot{\boldsymbol{u}} \\ \ddot{\boldsymbol{\phi}} \end{bmatrix} + \begin{bmatrix} K_{uu} & K_{u\phi} \\ K_{u\phi}^{T} & K_{\phi\phi} \end{bmatrix}\begin{bmatrix} \boldsymbol{u} \\ \boldsymbol{\phi} \end{bmatrix} = \begin{bmatrix} \boldsymbol{0} \\ \boldsymbol{0} \end{bmatrix} \tag{5}$$

Equation (3) is transformed as follows by the eigenvalue $[\omega_1, \ \cdots \ , \omega_m]$ and the eigen mode $\boldsymbol{\Psi} = [\boldsymbol{\psi}_1, \ \cdots \ , \boldsymbol{\psi}_m]$.

$$\begin{bmatrix} \ddot{\xi}_1 \\ \vdots \\ \ddot{\xi}_m \end{bmatrix} + \begin{bmatrix} \omega_1 & & \\ & \ddots & \\ & & \omega_m \end{bmatrix}\begin{bmatrix} \xi_1 \\ \vdots \\ \xi_m \end{bmatrix} = \begin{bmatrix} \boldsymbol{\psi}_1^{\boldsymbol{T}}\boldsymbol{F}_e \\ \vdots \\ \boldsymbol{\psi}_m^{\boldsymbol{T}}\boldsymbol{F}_e \end{bmatrix} + \begin{bmatrix} \boldsymbol{\psi}_1^{\boldsymbol{T}}\boldsymbol{F}_s \\ \vdots \\ \boldsymbol{\psi}_m^{\boldsymbol{T}}\boldsymbol{F}_s \end{bmatrix} \tag{6}$$

Where:

$$\boldsymbol{\xi} = [\xi_1 \quad \cdots \quad \xi_m]^T, \ \begin{bmatrix} \boldsymbol{u} \\ \boldsymbol{\phi} \end{bmatrix} = \boldsymbol{\Psi\xi}, \ \boldsymbol{F_e} = \begin{bmatrix} -K_{u\bar{\phi}}\bar{\boldsymbol{\phi}} \\ -K_{\phi\bar{\phi}}\bar{\boldsymbol{\phi}} \end{bmatrix}, \ \boldsymbol{F_s} = \begin{bmatrix} \boldsymbol{F} \\ \boldsymbol{0} \end{bmatrix}$$
$$\boldsymbol{F_{me}} = \begin{bmatrix} \boldsymbol{\psi_1^T F_e} \\ \vdots \\ \boldsymbol{\psi_m^T F_e} \end{bmatrix}, \ \boldsymbol{F_{ms}} = \begin{bmatrix} \boldsymbol{\psi_1^T F_s} \\ \vdots \\ \boldsymbol{\psi_m^T F_s} \end{bmatrix} \tag{7}$$
$$\boldsymbol{\Psi}^T \begin{bmatrix} M & 0 \\ 0 & 0 \end{bmatrix} \boldsymbol{\Psi} = \begin{bmatrix} \mathbf{I} & \\ & \mathbf{0} \end{bmatrix}, \quad \boldsymbol{\Psi}^T \begin{bmatrix} K_{uu} & K_{u\phi} \\ K_{u\phi}^T & K_{\phi\phi} \end{bmatrix} \boldsymbol{\Psi} = \begin{bmatrix} \omega_1 & & \\ & \ddots & \\ & & \omega_m \end{bmatrix}$$

$\boldsymbol{\xi}$ is the modal coordinate coefficient. The degree of freedom of stator can be substantially decreased by mode reduction.

3.4. Rotor modelling and contact problem

Simulation of rotating the FEM mesh by contact friction becomes a nonlinear transient analysis that takes into account the finite deformation and the simulation requires a lot of time. Therefore, it is proposed to consider the rotor as the one degree of freedom (DOF) rigid body, or the two DOF model with the twist spring. By modelling of such rotor, rotation of the FEM mesh is eliminated. Thus, nonlinearity is taken into consideration contact only. Then, the calculation time is greatly reduced.

In this paper, the rotor is regarded as a two DOF model with twist spring and damper. When the rotor is the one DOF model of rigid body, the response of its rotational speed is faster compared with the results of FEM [7]. Therefore, the rotor is assumed to be the secondary delay system and the two DOF model.

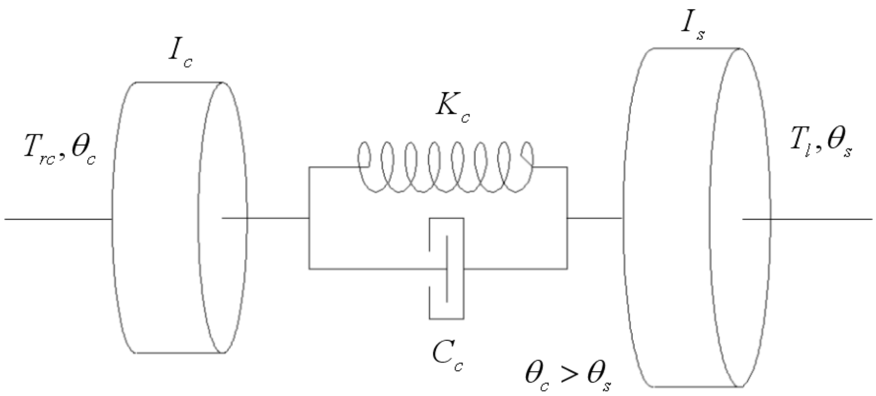

Figure 4. The rotor as an elastic body of two DOF model.

Figure 4 is the two DOF model illustrated schematically. The model has a torsion spring and a damping between the two inertia. Equation (8) is the equation of motion of the rigid body as one DOF model.

$$I_r\ddot{\theta}_r = T_{rc}$$
$$T_{rc} = \mu \sum_{i=1}^{n} \Delta F_{rc} \tag{8}$$

Where, μ is coefficient of friction, and ΔF_{rc} is the friction force of contact. Equation (9) is the equation of motion of the two DOF model shown in figure 4.

$$\begin{cases} I_c\ddot{\theta}_c = -C_c(\dot{\theta}_c - \dot{\theta}_s) - K_c(\theta_c - \theta_s) + T_{rc} \\ I_s\ddot{\theta}_s = -C_c(\dot{\theta}_s - \dot{\theta}_c) - K_c(\theta_s - \theta_c) + T_l \\ I_r = I_c + I_s \end{cases} \tag{9}$$

Where, I_r , I_c and I_s are inertia. K_c is twist spring constant. C_c is twist damping coefficient. The problem becomes to determine the parameters (I_c,I_s,K_c,C_c). These parameters are determined in the following way.

1. The drive torque and rotor's results ($\ddot{\theta}_r, \dot{\theta}_r, \theta_r$) using the 1DOF rigid rotor model and reduced order stator model obtains.
2. Obtained drive torque and rotor's results ($\ddot{\theta}_r, \dot{\theta}_r, \theta_r$) are substituted into T_{rc} and $\ddot{\theta}_s, \dot{\theta}_s, \theta_s$ of equation (9).
3. I_c, C_c, K_c is obtained by minimizing the difference between $\ddot{\theta}_r, \dot{\theta}_r, \theta_r$ and $\ddot{\theta}_c, \dot{\theta}_c, \theta_c$.

$$\min:\{(\ddot{\theta}_r - \ddot{\theta}_c) + (\dot{\theta}_r - \dot{\theta}_c) + (\theta_r - \theta_c)\}$$

$$\text{subject:}\begin{cases} I_c\ddot{\theta}_c = -C_c(\dot{\theta}_c - \dot{\theta}_r) - K_c(\theta_c - \theta_r) + T_{rc} \\ I_r\ddot{\theta}_r = -C_c(\dot{\theta}_r - \dot{\theta}_c) - K_c(\theta_r - \theta_c) \\ I_r = I_c + I_s \end{cases} \tag{10}$$

$$\text{find: } I_c, C_c, K_c$$

Equation (10) is determined by the nonlinear least-squares method of MATLAB Optimization toolbox.

4. Using the determined parameters I_c,I_s,K_c,C_c, simulation of the two DOF rotor model and reduced order stator model performs.

Table 6 shows parameters of two DOF model obtained through the process from above 1 to 4.

Table 6. Determined parameters of two DOF rotor model

	Inertia (kg·m^2)
I_c	8.1006E-6
I_s	8.8994E-6
I_r	1.7E-5

	spring constant (N·m/rad)
K_c	0.299

	attenuation coefficient (N·m·sec/rad)
C_c	0.0024

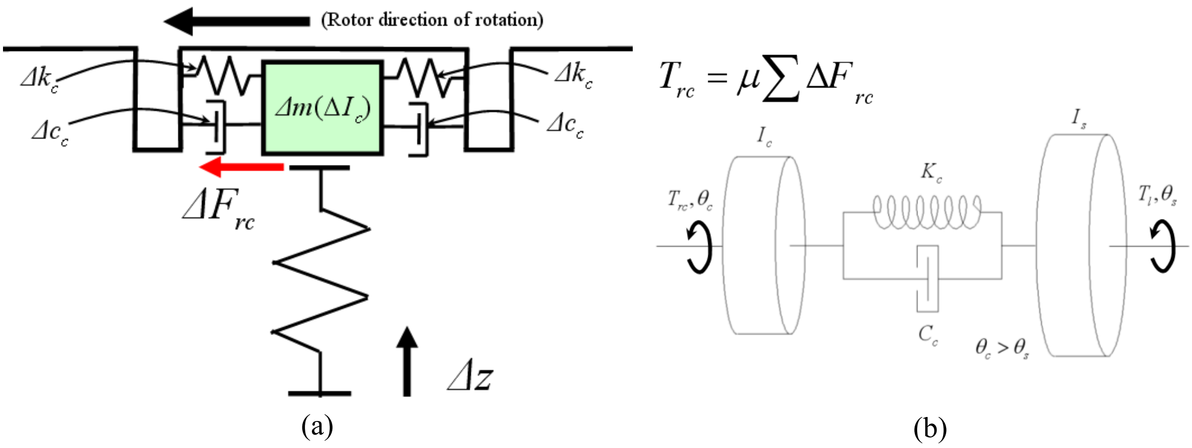

Figure 5. Contact model image and the two DOF rotor model

In figure 5 (b), I_c can be interpreted as the set of mass ($\Delta m(\Delta I_c)$) which receives the power (ΔF_{rc}) in figure 5 (a), and $K_c$and C_c of figure 5 (b) are also interpreted as the set of the stiffness (Δk_c) and the damping (Δc_c) acting on the mass$\Delta m(\Delta I_c)$.

3.5. State-space realization model

Figure 6 shows the state from which frictional force by ultrasonic vibration of stator is transmitted to rotor typically. The contact interaction of the rotor and the stator is considered in the model [8]. The nonlinear part is separated from linear part. Model reduction is applied to each part. Equation (6) and (9) are rewritten in the following state-space realization.

$$\begin{cases} \dot{\boldsymbol{x}}_s = A_s \boldsymbol{x}_s + B_s \boldsymbol{u}_e + B_s \boldsymbol{u}_f \\ \boldsymbol{y}_s = C_s \boldsymbol{x}_s \end{cases} \tag{11}$$

Where:

$$\boldsymbol{x}_s = \begin{bmatrix} \xi \\ \dot{\xi} \end{bmatrix},\ \boldsymbol{u}_e = \begin{bmatrix} \mathbf{0} \\ \boldsymbol{F}_{me} \end{bmatrix},\ \boldsymbol{u}_f = \begin{bmatrix} \mathbf{0} \\ \boldsymbol{F}_{ms} \end{bmatrix},\ A_s = \begin{bmatrix} & \mathbf{0} & & \boldsymbol{I} \\ \omega_1 & & & \\ & \ddots & & \mathbf{0} \\ & & \omega_m & \end{bmatrix},\ B_s = \begin{bmatrix} \mathbf{0}_m & \boldsymbol{I}_m \\ \mathbf{0}_m & \mathbf{0}_m \end{bmatrix},\ C_s = [\Gamma \quad \mathbf{0}] \tag{12}$$

and Γ in $C_s$of equation (10)

$$\Gamma = U\boldsymbol{\Psi} \tag{13}$$

Where, U is a rectangular unit matrix of the output number by whole degree of freedom. The value of the column of an output point is one, and all the others is zero.

$$\begin{cases} \dot{\boldsymbol{x}}_r = A_r \boldsymbol{x}_r + B_r \boldsymbol{u}_{rf} \\ \boldsymbol{y}_r = C_r \boldsymbol{x}_r \end{cases} \tag{14}$$

Where:

$$\boldsymbol{x}_s = \begin{bmatrix} \theta_c \\ \theta_s \\ \dot{\theta}_c \\ \dot{\theta}_s \end{bmatrix},\ A_r = \begin{bmatrix} 0 & 0 & 1 & 0 \\ 0 & 0 & 0 & 1 \\ -K_c I_c^{-1} & K_c I_c^{-1} & -C_c I_c^{-1} & C_c I_c^{-1} \\ K_c I_s^{-1} & -K_c I_s^{-1} & C_c I_s^{-1} & -C_c I_s^{-1} \end{bmatrix},\ B_r = \begin{bmatrix} 0 & 0 \\ 0 & 0 \\ I_c^{-1} & 0 \\ 0 & I_s^{-1} \end{bmatrix},\ C_r = \begin{bmatrix} 0 & 0 & 1 & 0 \\ 0 & 0 & 0 & 1 \end{bmatrix} \tag{15}$$

$$\boldsymbol{u}_{rf} = \begin{bmatrix} T_{rc} \\ T_l \end{bmatrix}$$

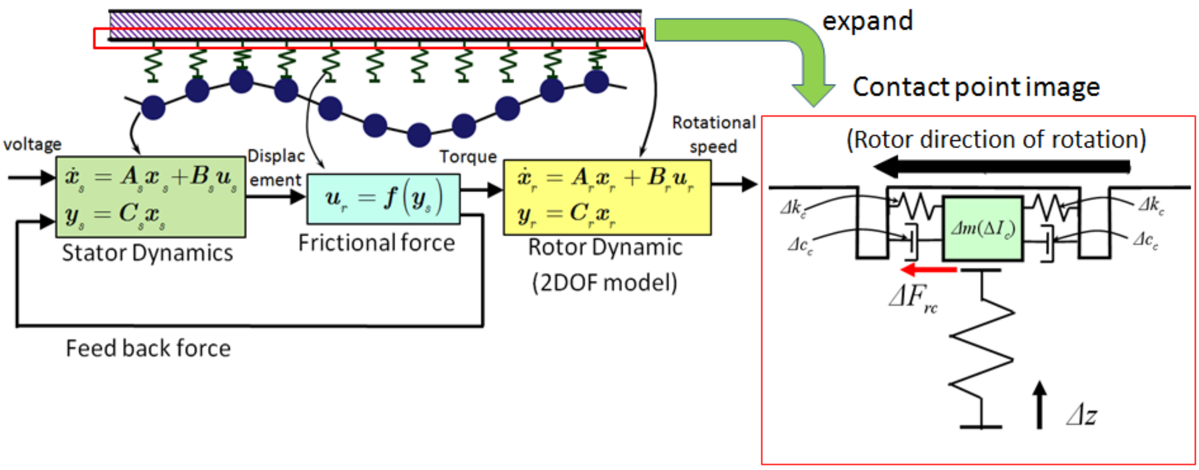

Figure 6. Reduced order model of USM

4. Numerical Experiments of FEM model and reduced order model

4.1. Comparison on result and computing time

The effect of the proposed model is indicated by USM simulation. Figure 7 shows the graph comparing the rotational angle and the rotational speed of the rotor. The blue line shows the FEM result. The pink line shows the results of the proposed reduced order model.

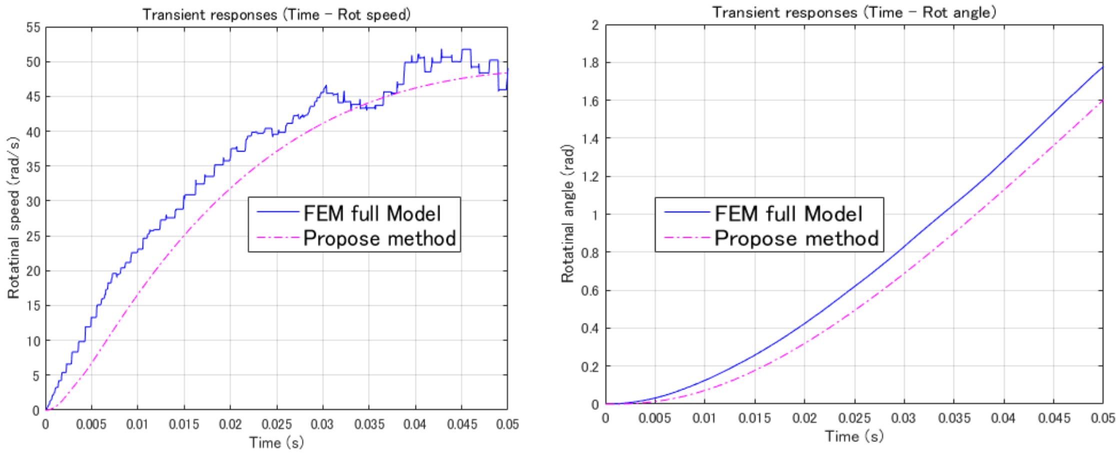

(a) (b)

Figure 7. Simulation results (a) angular speed and (b) angle

Table 7. Computational time

Proposed technique (sec)	FEM analysis (sec/hour)
263	225,128/62.5

Table 7 shows the computation time. Computation time of the proposed method has been greatly reduced. Simulation time is 50msec.

5. Speed follow-up control using Nonlinear Model Predictive Control

5.1. Developing a plant model for NMPC controller

This section introduces the nominal model for applying the NMPC. The rotational speed of the USM is assumed as an expression of the following first order delay system.

$$G(s) = \frac{K}{Ts + 1} \quad (16)$$

K and T of the first order delay system are dependent on Voltage and Load.

$$G(s) = \frac{K(v,l)}{T(v,l)s + 1} \quad (17)$$

It becomes the nonlinear function which depends on the driving voltage and the load. The values of Table 7 and Table 8 are Gain constant and Time constant. They are determined by the least squares method.

Table 8. Gain constant

		Voltage (V)				
		50	75	100	125	150
	0	15.3971	30.8797	37.1949	49.2783	60.1403
Load	0.04	9.5262	21.8862	34.4566	38.3776	46.8492
(N·m)	0.08	3.8181	9.6119	22.4938	27.1059	38.1937
	0.12	0	1.2442	3.6185	11.6298	22.93
	0.16	0	0	0	0	0

Table 9. Time constant

		Voltage (V)				
		50	75	100	125	150
	0	0.0035	0.0047	0.0045	0.0058	0.0065
Load	0.04	0.0031	0.0049	0.0068	0.0059	0.0075
(N·m)	0.08	0.0026	0.003	0.0078	0.0079	0.0105
	0.12	0	0.0028	0.0038	0.0149	0.0245
	0.16	0	0	0	0	0

The values of the Table 8 and Table 9 are fitted to the polynomial shown equation (18) and (19). Fitting is using the least squares method of MATLAB.

$$K(l,v) = a_1 + a_2 l + \cdots + a_{n-1} l v^3 + a_n v^4 \tag{18}$$

$$T(l,v) = b_1 + b_2 l + \cdots + b_{n-1} l v^3 + b_n v^4 \tag{19}$$

In order to confirm the controller performance, it gives the variation in voltage and load. Where v is the driving voltage, and l is the load. Voltage and load are given as follows.

$$l = 0.01\sin(\omega t) + 0.08 \tag{20}$$

$$v = 10\sin(\omega t) + 125 \tag{21}$$

Where, $\omega = 1800$ (rad/sec) is angular velocity.

5.2. Application of NMPC controller to nominal model

The nonlinear state space equation from the nonlinear function determined at the previous subsection and composed NMPC control system is derived. The voltage which can be input is subject to restrictions, so it is the constrained optimal control problem. NMPC formulation is as follows [9].

$$\begin{aligned} &\dot{\boldsymbol{x}}(t) = \boldsymbol{f}(\boldsymbol{x}(t), \boldsymbol{u}(t), \boldsymbol{p}(t)) \\ &J := \varphi(\boldsymbol{x}(t+T), \boldsymbol{p}(t+T)) + \int_t^{t+T} L(\boldsymbol{x}(\tau), \boldsymbol{u}(\tau), \boldsymbol{p}(\tau))d\tau \\ &C(\boldsymbol{x}(t), \boldsymbol{u}(t), \boldsymbol{p}(t)) = 0 \end{aligned} \tag{22}$$

Where, $\dot{\boldsymbol{x}}(t)$ is state vector, $\boldsymbol{u}(t)$ is control input vector, and $\boldsymbol{p}(t)$ is reference vector. J is a performance index. φ is called a terminal cost and L is called a stage cost. C is a constraint condition. The first order delay system of the ultrasonic motor is applied to these NMPC formulations. They are expressed as follows.

$$
\begin{aligned}
\dot{x}(t) &= -\frac{1}{T(l,v)}\left(x(t) - \frac{K(l,v)u_1(t)}{Load}\right) \\
J &:= \varphi + \frac{1}{2}\int_t^{t+T} \left\{\left(x(t) - p(t)\right)^2 Q_1 - g_1 u_2\right\} d\tau \\
C &= (u_1 - \bar{u})^2 + u_2^2 - (u_{max} - \bar{u})^2 = 0, \quad \bar{u} = \frac{u_{max}+u_{min}}{2}
\end{aligned} \tag{23}
$$

Where, u_2 is called a slack variable. u_{max} is maximum control input value, and u_{min} is minimum control input value. $\varphi = 10^{-6}$, $p(t) = 27.1$, $Q_1 = 1.0$, $g_1 = 0.5$. The NMPC Algorithm is described on commercial software Maple.

5.3. Automatic Controller Generation System

It has to automatically generate code by Maple formula processing functions. It shows the control result due to the controller is shown in figure 8. In figure 8, (a) is a rotational speed of the rotor. (b) is a torque. The rotational speed is closed to the target value well.

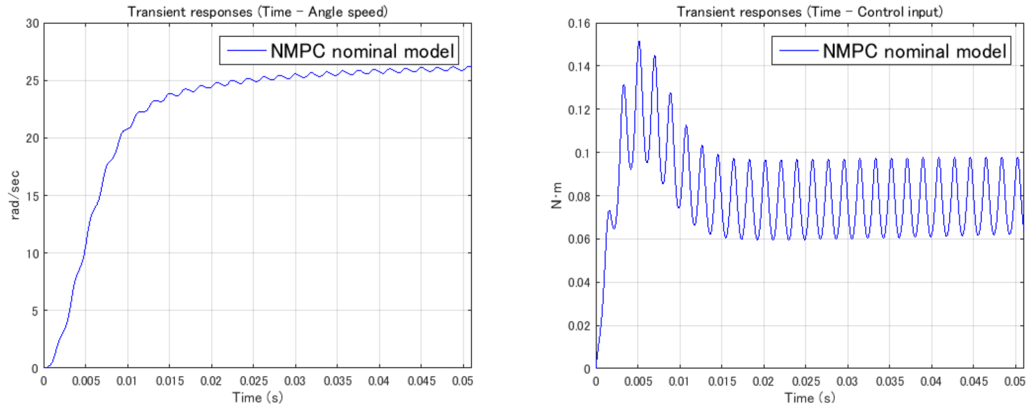

(a) (b)

Figure 8. Nominal model result

5.4. Application of the NMPC controller to reduced order model

Figure 9 shows the result obtained by applying NMPC controller to the rotor of proposed reduced order models. In Figure 9, (a) shows the rotational speed of the reduced order rotor model, and (b) shows torque. The rotation speed is closed to the target value.

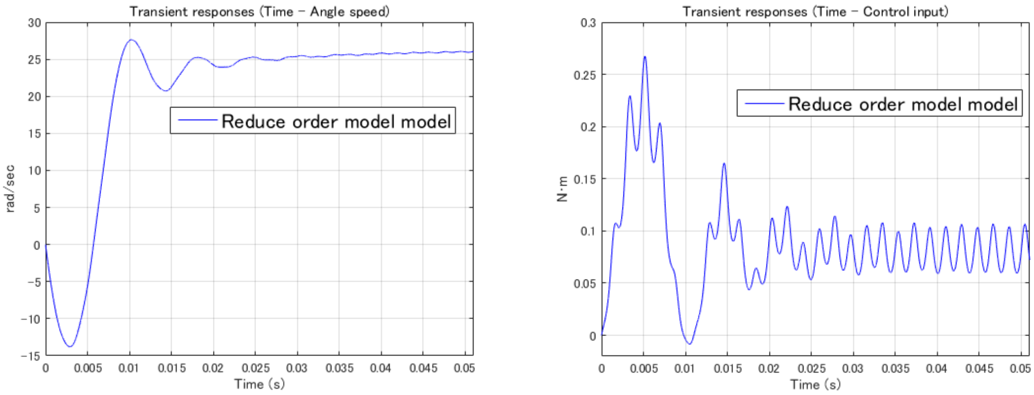

(a) (b)

Figure 9. Reduced order model result

6. Conclusion

In this paper, the method of constituting the control system after deriving a control model systematically from FEM accurate model of USM is shown.

The reduced order model is introduced before deriving the nominal model for control. Then, identification of nominal model using proposed reduced order model is performed. By simulation, the performance of the NMPC controller has been confirmed. It has to save time significantly than deriving a control model from the results of FEM. One method for performing ultrasonic motor design quickly has been shown.

7. Future work

The accuracy of the reduced order model is improved. More specifically, the reduced order model is improved to be able to get the current. Then, it is improved so that it can be applied to the controller to the whole reduced order model.

References

[1] Kenjo T and Sashida T 1994 *An Introduction to Ultrasonic Motors* (Oxford University Press)

[2] Maeno T, Tukimoto T, and Miyake A 1992 *IEEE Trans. Ultrasonic, Ferroelectric, and Freqency Control.* **39**-6 pp 668-674.

[3] El Hagry M T, Mahfouz A A, and Ahmed H S 2005 *ACMOS'05 Proceedings of the 7th WSEAS international conference on Automatic control, modeling and simulation* pp 472-481.

[4] Ohtsuka T 2004 *Automatica* **40**-4 563-574.

[5] Mitani A and Akishita S 2001 *Transactions of the Japan Society of Mechanical Engineers Series* C **67**-661 pp 2843-48.

[6] Kobayashi Y, Kimura T, and Yanabe S 1998 *Transactions of the Japan Society of Mechanical Engineers Series* C **64**-627 pp 4271-77.

[7] Miyauchi R, Matsunaga N and Ishizuka S 2014 *The 12th International Conference on Motion and Vibration* (Sapporo Hokkaido)

[8] Marchesillo S and Garibaldi L 2008 *Mechanical System and Signal Processing* **22**-1 81-101.

[9] Ohtsuka T 2011 *Introduction to Nonlinear Optimal Control* (CORONA PUBLISHING CO., LTD) chapter 5 pp 102-120